Available online at www.sciencedirect.com

ScienceDirect

Procedia Engineering 72 (2014) 636 – 641

Procedia Engineering

www.elsevier.com/locate/procedia

The 2014 conference of the International Sports Engineering Association

Stress analysis of bicycle saddles structural components during different cycling conditions.

Federico Giubilato[a*] , Nicola Petrone[a]

a Department of Industrial Engineering, University of Padova, Via Venezia 1, 35131 Padova, Italy

Abstract

The structural behaviour of a bicycle saddle is mainly affected by the shell and the rails properties and by their assembly connections. The knowledge of the stress acting on these components is therefore fundamental for a safe and performing saddle engineering design. The aim of the work was the measurement and analysis of the strain/stress state of shell and rails of a bicycle saddle during real cycling conditions. The shell and the rails of a saddle were instrumented with a total of 16 strain gauge channels, allowing the measurement of the local deformations of shell and rails. Two field test sessions (one for road cycling and one for mountain bike riding) were performed with two professional cyclists different for body height and weight (65 and 76 kg). Reported results regard the analysis of rails cyclic stresses due to road pedalling and of stress cumulative spectra obtained during road and mountain bike sessions. Right and the left portions of the rails were loaded symmetrically. The two testers showed large differences in the pedalling style and in the cycling posture. The stress on the front and rear rails portions was mainly influenced by the cyclist posture and pedalling style. An increase of the road slope caused an increment of the stress range and mean values; the damage ratio between mountain bike and road load spectra for an equivalent cycled distance resulted to range between 6 and 9, depending on the tester involved.

Selection and peer-review under responsibility of the Centre for Sports Engineering Research, Sheffield Hallam University

"Keywords: Bicycle saddle; strain gauges; stress analysis; road cycling;"

* Corresponding author. Tel.: 3409704760.
E-mail address: mail@federicogiubilato.com

Selection and peer-review under responsibility of the Centre for Sports Engineering Research, Sheffield Hallam University
doi:10.1016/j.proeng.2014.06.103

1. Introduction

The behaviour of bicycle saddle has been already studied in the past in terms of field load acquisition (Petrone et al., 1996; Seragio et al., 2004) and correlation with perceived comfort (Stone & Hull, 1995; Petrone & Giubilato, 2013), in analogy with other components like frames (Hastings et al., 2004) and handlebars (Petrone & Susmel, 2003). The trend of modern bicycle saddles towards the lowest mass and minimal structures justifies again the interest towards the comprehension and evaluation of the saddle components structural behaviours during cycling.

A bicycle saddle is usually composed by an upper shell, covered by a soft padding and a top cover, giving the external shape to the saddle, constrained at the tail and the nose to the rails which are clamped to the seat post within their straight portion. The structural behaviour of a saddle is affected by the shell and the rails properties and by their assembly connections. These factors influence the saddle comfort behaviour, its compliance, its strength and fatigue life. The knowledge of the stress acting on these components is therefore fundamental for the saddles design.

The aim of the present work was the measurement and the analysis of the strain/stress state of the shell and the rails of a bicycle saddle during real cycling conditions, after involving two expert testers during extensive field data collection in road and mountain bike sessions.

2. Method

2.1. Instrumentation

A saddle suitable for both racing and mountain bike was selected for the study. The right and the left straight portions of the steel rails were instrumented with 12 strain gauges placed on two opposite locations away from the saddle clamp zone (Fig. 1.a). Eight strain gauge channels were defined with different connection schemes: four quarter bridges (ch1, ch2, ch3, ch4), two half bridges for the measurement of the strain due to bending moment (ch5, ch6), one full bridge for the measurement of the strain due to twisting moment (ch7) and one full bridge for the measurement of the axial stress (ch8).

Four uniaxial (Kyowa KFG-2N-120-C1-16-L3M2R) and two biaxial (Kyowa KFG-2-120-D16-23) strain gauges were placed in different positions on the shell bottom surface (Fig. 1.b). Five strain gauges were placed along the shell longitudinal mean line (x-axis), one biaxial strain gauge was placed laterally at the shell widest section at a distance of y = 40 mm from the longitudinal mean line. All the strain gauges were connected adopting the quarter bridge scheme and obtaining in this way a total of eight channels. The system of reference adopted for the shell has its origin at a distance of 230 mm from the rails/shell front inner contact point.

The strain values measured by the rails channels were combined following the relationships showed in Fig. 4. The resulting deformation values were attributed to a new set of channels called *virtual channels*.

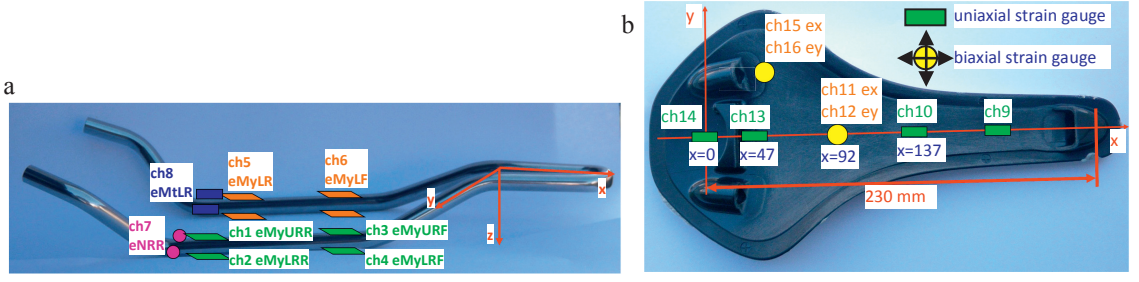

Fig.1 Schematic of the rails (a) and shell (b) strain gauges placement and denomination.

The nomenclature adopted for the strain gauge channels and for the virtual channels is showed in figure 3. Each channel name is divided in three parts: the first part (1) indicates whether the channel refers to a strain gauge or a

virtual channel, the second one (2) indicates the parameter generating the strain measured, the third one (3) indicates the channel placement.

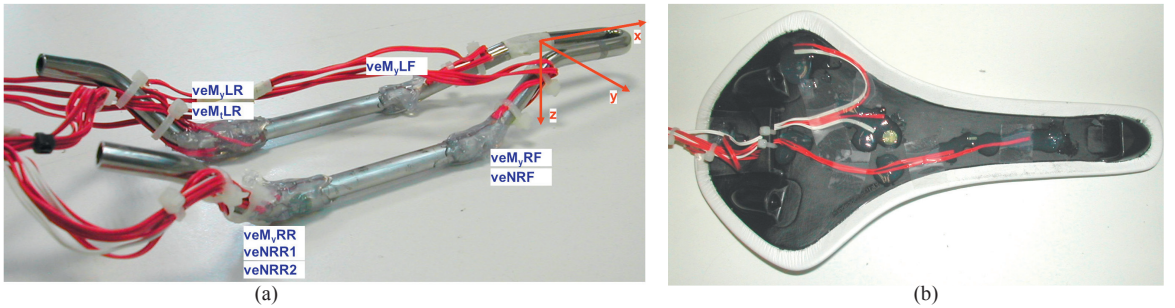

(a) (b)

Fig.2 View of the instrumented rails (a) and shell (b).

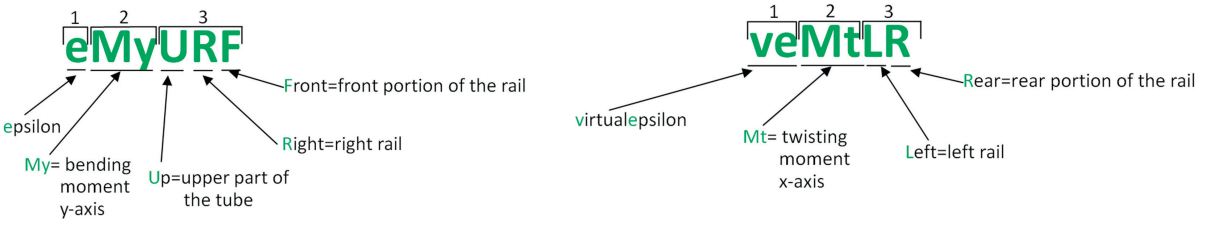

Fig. 3 Schematic of the nomenclature adopted for the strain gauge and virtual channels.

Chan Nr.	strain gauge chan_id
1	eMyURR
2	eMyLRR
3	eMyURF
4	eMyLRF
5	eMyLR
6	eMyLF
7	eNRR
8	eMtLR

Chan Nr.	virtual chan_id	formulation
1	veMyRR	veMyRR = (eMyURR – eMyLRR)/2
2	veNRR2	veNRR2 = (eMyURR + eMyLRR)/2
3	veMyRF	veMyRF = (eMyURF – eMyLRF)/2
4	veNRF	veNRF = (eMyURF + eMyLRF)/2
5	veMyLR	veMyLR = eMyLR/2
6	veMyLF	veMyLF = eMyLR/2
7	veNRR1	veNRR1= eNRR
8	veMtLR	veMtLR = eMtLR

Fig. 4 Relationships between the rails strain gauge channels and the virtual channels.

For the conventions adopted, the shell strain values and veN channel were assumed positive for a tensile deformation, the rails veMy channels were positive when upper fibers were in tension.

2.2. Rails and shell calibration

Three different types of pure loads, represented by the bending moment My, the axial load N and the twisting moment Mt, were applied to the front and the rear part of both the right and the left rails portion during the calibration tests (Fig. 5.a, 5.b). The constants which express the relationship between each virtual channel and the relative load case were calculated in order to verify that all the rails channels were correctly functioning and sufficiently decoupled. During the field tests, after the saddle assembly, the rails could not be used as a load cell due to the hyper static behaviour of the constraint system between the shell and the rails.

The shell was calibrated after applying a vertical load at a distance of 110 mm from the tip, with the shell

simply supported at the tail and the tip (Fig. 5.c). The resulting shell deformation involved a global tensile strain of the longitudinal mean line. The shell calibration results, visible in Fig. 5.d, are represented by the sensibility constants that relate each channel to the load applied. The negative longitudinal strain values obtained for the channels at x = 47 mm and x = 92 mm are due to the biaxial global deformation of the shell whose transverse component heavily affects the longitudinal strain measured.

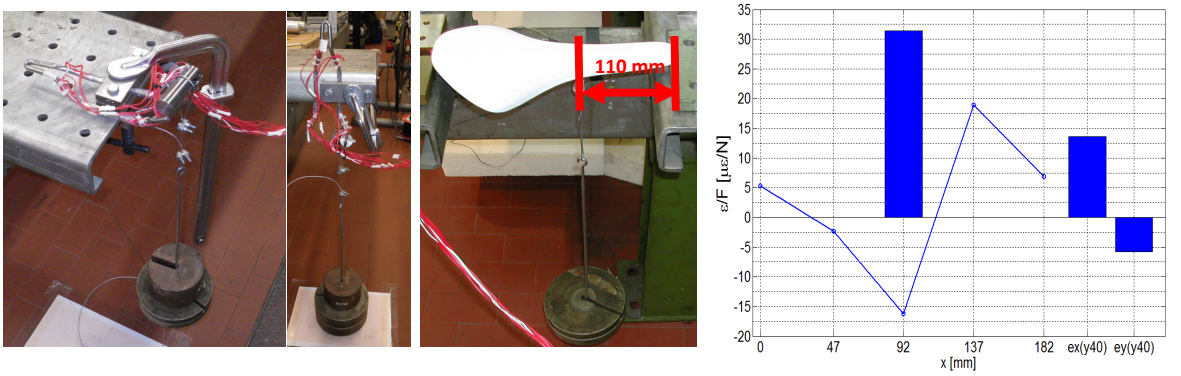

(a) (b) (c) (d)

Fig. 5. (a) Pure bending moment calibration of the right rear rail portion. (b) Pure normal load applied to the right rear rail portion. (b) Shell bending calibration. (c) Sensibility constants calculated for the shell channels. *Line*: sensibility constant calculated for the longitudinal strain channels along the x-axis. *Bar at x=92*: sensibility constant calculated for the transverse strain measured on the x-axis at x=92 mm. *Bar ex(y40), ey(y40)*: sensibility constant calculated respectively for the x and y strain measured by the strain gauge placed laterally at y=40 mm.

2.3. Field test sessions

Two field test sessions, road and mountain bike (MTB), were performed for measuring the saddle strain/stress state during real cycling conditions. The road and MTB testing paths, respectively 15.5 and 12.5 km long with 260 and 200 m altitude gap gradient, were selected in order to reproduce most of the typical situations encountered during road and mountain bike cycling, in analogy with former experiences (Seragio et al., 2004). Two professional cyclists took part in both the road and MTB test sessions. They were selected to have different body height and weight: Tester 1, 1.65 m tall, 65 kg mass, Tester 2, 1.95 m tall, mass 76 kg. During the test sessions each tester had to ride once the road and once the MTB path with the instrumented saddle assembled to its own bicycle. The strain gauge channels were recorded by means of a SoMat eDaq Lite data acquisition system at a sampling rate of 1000 Hz. A Garmin EGPS-5HZ GPS was also used during the tests for recording the bicycle cruising speed, the altitude and the cyclist position along the path.

2.4. Data analysis

Data analysis focused mainly on the rails virtual channels signals. For each typical action performed by the tester during the rides, e.g. the cycling on flat road, uphill, downhill, pothole or bumps etc., the different stress sources were identified and separately analysed. For each typical action, three types of stress were identified: the stress due to the pedalling action, the stress due to impacts and the stresses due to vibrations.

A fatigue analysis was also performed after calculating the rainflow counting of the collected field load histories from the road and mountain bike field collected data.

3. Results and Discussion

All the collected data showed that stresses due to axial loads and twisting moment were negligible with respect to stresses due to bending moment. The left and right rail portions were symmetrically loaded by both testers.

The rails cyclic strain due to the pedalling action is represented in Fig. 6.a. Deformation of the right and left

rails front portions (veMyRF, veMyLF) are overlapping. The right and the rear portions of the rails (veMyRR, veMyLR) reach the same deformation values with a half period phase shift. During a complete pedalling cycle, represented by two subsequent strokes on pedals with the left and the right leg, the phase corresponding to the stroke on the pedal produces a valley of the front channels and a peak of the rear channels which is maximum for the channel of the rails portion closer to the pushing leg, e.g. left rear channel for the left pushing leg. The phase corresponding to the transfer between two consecutive strokes on pedals produces a peak of the front channels and a coincident valley of the rear channels.

The comparison between the cyclic strains measured for the two testers, while they were cycling through the same test path section, shows that Tester 2 (mass 76 kg) is seated in a more forward position than Tester 1 (65 kg mass). The pedalling action of Tester 1 resulted symmetric; an asymmetric behaviour is showed by Tester 2 whose stroke on pedal with the right leg produces two coincident peaks on both the right and the left rear portions. This aspect can be explained by the cyclist tendency to pull the left pedal while pushing on the right leg.

The max/min/range values of the strain cycles calculated for Tester 1, averaged over 20 strokes on pedals, are showed in figure 6.b: the different actions performed during the road field test are described at the front (veMyRF) and the rear (veMyRR) right rails portions. The rails stress during flat road cycling, flat road cycling on city paved surface and low slope uphill cycling are similar. The increase of the road slope produces an increment of the stress range and of the respective mean value; the pedalling action on steep slope uphill causes the rails maximum stress.

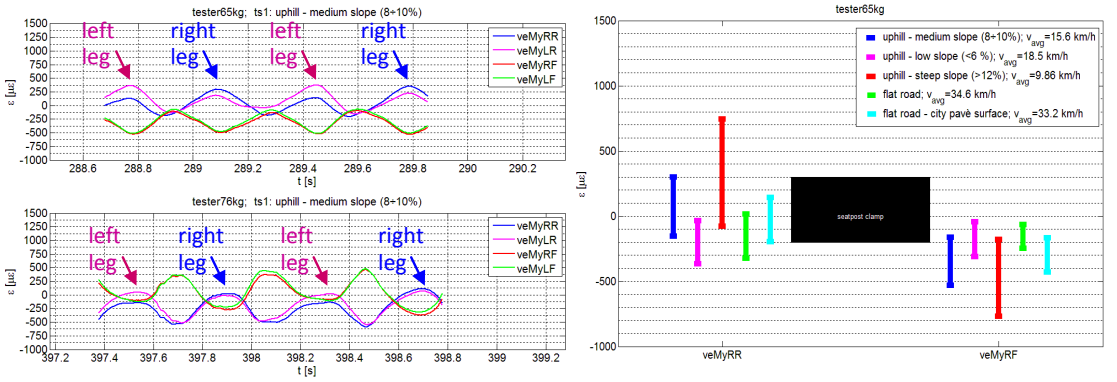

(a) (b)

Fig. 6. (a) Example of rails cyclic deformation due to two complete pedaling cycles; (b) max/min/range values of the cyclic strain measured for Tester 1 (65 kg) in the different actions performed during the road field tests.

An example of rainflow counting results in shown in Fig. 7.a as range-mean counting histograms, obtained for channel eMyURR after the MTB test of both testers. Higher number of cycles appears at stress cycles with lower amplitudes. Tester 1, 65 kg mass, showed a larger mean value than Tester 2, 76 kg mass. This was again due to the fact that Tester 1 was seated in a more rearward position on the saddle during the mountain bike riding, despite his shorter height.

A comparison between the cumulative stress spectra extended to a reference distance of 10000 km, calculated for the two testers during the road and MTB tests is reported in Fig. 7.b. The cumulative stress spectra obtained from the MTB tests show consistently higher amplitudes which correspond to higher rails fatigue damage or lower fatigue life, when compared to an engineering fatigue Wohler curve estimated for the rail material. For Tester 1, the fatigue damage calculated from the MTB field data resulted to be 6 times larger than the damage obtained after the road tests; for Tester 2, this ratio increases to a value of 9. This high difference is however compensated by the usual shorter mission associated to 10 years of MTB amateur usage (40000 km) than of road use (100000 km).

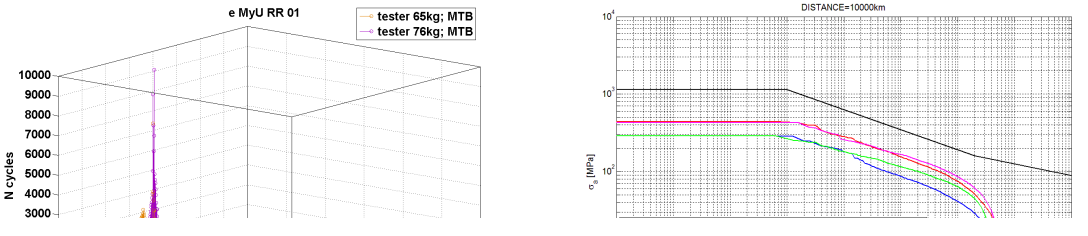

(a) (b)

Fig. 7. (a) Example of rainflow counting results on strain gauge channel 1 eMyURR, from MTB, Tester 1 & 2; (b) cumulative stress spectra resulting from road and MTB data collection, extended to 10000 km at channel eMyURR for Tester 1 and channel eMyURF for Tester 2.

4. Conclusions

The proposed method described the location, combination and calibration of strain channels applied to the rails and the shell of a modern saddle in order to collect field data during representative road and mountain bike sessions. Results revealed the strong influence of rider posture rather than rider mass on stress states and on the fatigue damage ratio between mountain bike and road stress spectra.

Acknowledgements

The work was supported by Selle Royal S.p.a. - Italy.

References

Hastings A.Z., Blair K.B., Culligan F.K., Pober D.M., Measuring the effect of transmitted road vibration on cycling performance, The Engineering of Sport 5, Davis, 2004.

Petrone N., Giubilato F, 2011, Methods for evaluating the radial structural behaviour of racing bicycle wheels, The 5th Asia Pacific Congress on Sports Technology, Procedia Engineering, Volume 13, pages 88-93.

Petrone N., Giubilato F., 2013, Development of a Test Method for the Comparative Analysis of Bicycle Saddle Vibration Transmissibility, Procedia Engineering, Volume 60, pages 288-293

Petrone N., Susmel L., Biaxial Testing and Analysis of Bicycle-Welded Components for the Definition of a Safety Standard, Fatigue and Fracture of Engineering Material and structures, 26, 491-505, Blackwell Publishing Ltd., UK, 2003

Petrone N., Tessari A., Tovo R., 1996, Acquisition and analysis of service load histories in mountain-bikes, XXV° Convegno Nazionale AIAS, International Conference on Material Engineering, Gallipoli - Lecce, 4-7 September 1996, pp. 851-858.

Seragio E., Petrone N., Marchiori M., 2004, Design and calibration of a dynamometric saddle support for racing and mountain bikes , Proceedings of 5th International Conference on the Engineering of Sport, University of California, Davis, 13-16 September 2004, Vol. 2, pp. 187-193, ISBN 0-9547861-1-4.

Stone C., Hull M.L., Effect of rider weight on rider-induced loads during common cycling situations, Journal of Biomechanics, 28 (4), 365-375.